NACA RM A58D15

NACA

RESEARCH MEMORANDUM

EXPERIMENTAL INVESTIGATION OF THE DRAG DUE TO WEDGES ALONG THE TRAILING EDGE OF A SWEPT WING

By Bruno J. Gambucci and John A. Wyss

Ames Aeronautical Laboratory
Moffett Field, Calif.

NATIONAL ADVISORY COMMITTEE
FOR AERONAUTICS

WASHINGTON
June 27, 1958
Declassified January 12, 1961

NATIONAL ADVISORY COMMITTEE FOR AERONAUTICS

RESEARCH MEMORANDUM

EXPERIMENTAL INVESTIGATION OF THE DRAG DUE TO WEDGES ALONG THE TRAILING EDGE OF A SWEPT WING

By Bruno J. Gambucci and John A. Wyss

SUMMARY

A wind-tunnel investigation was conducted to determine the drag increment due to the superposition of wedges with various plan-form shapes along the trailing edge of a sweptback wing. Data were obtained at a model angle of attack of 0° and a Mach number range of 0.60 to 1.15. Reynolds number varied from 6,000,000 to 7,000,000.

Trailing-edge wedges similar to two sets reported on herein have been used on the control surfaces of unswept wings to alleviate or eliminate unstable aerodynamic damping at subsonic Mach numbers. All the trailing-edge wedges tested increased the drag over that of the basic wing-body combination. Drag computations indicated the possibility of reducing the transonic drag rise by contouring the body.

INTRODUCTION

The investigation reported in reference 1 revealed that triangular-shaped wedges placed on a control surface eliminated unstable aerodynamic damping and thereby prevented a single-degree-of-freedom flutter from occurring at subsonic speeds. However, an increase in environmental pressure fluctuations was observed, indicating that the wedges increased buffeting. Also, it is evident that drag penalties could be associated with the addition of the wedges. Because of the method of installation of the model for reference 1, drag measurements were not obtained. It is the purpose of this investigation to determine the magnitude of the drag penalty associated with various trailing-edge wedge configurations that may alleviate or eliminate control-surface flutter (see refs. 1 and 2). Data are presented for six trailing-edge modifications.

SYMBOLS

A	aspect ratio
c	local chord of wing measured parallel to plane of symmetry, ft
$\bar{c}$	mean aerodynamic chord
C_{D_o}	zero-lift drag coefficient, $\frac{D}{qS}$
D	drag, lb
M	free-stream Mach number
q	free-stream dynamic pressure, $\frac{1}{2}\rho V^2$, lb/sq ft
S	total wing area including the region within the body, sq ft
V	free-stream velocity, ft/sec
λ	taper ratio
ρ	mass density of air, slugs/cu ft

MODELS AND TESTS

Basic Model

The basic model is illustrated in figure 1. The wings had an aspect ratio of 3, a taper ratio of 0.4, a leading-edge sweep angle of 45.3°, and modified NACA 64A006 sections perpendicular to a line sweptback 39.45° which was the quarter-chord line of these sections. The body was a Sears-Haack body and had a closed fineness ratio of 12.5. A complete description of the wing-body combination is given in reference 3.

The model was mounted in the wind tunnel by means of a sting, and the drag force was measured as an electrical output from a strain-gage balance located within the model. A photograph of the model support system is shown in figure 2.

Drag force data are presented in this report for an angle of attack of 0°. The drag data were adjusted to the condition of zero base drag by use of the static pressures measured over the base of the body.

Data were obtained at Mach numbers ranging from 0.60 to 1.15. The corresponding Reynolds numbers based on the mean aerodynamic chord of the wing varied from about 6,000,000 to 7,000,000.

Trailing-Edge Modifications

Three basic types of trailing-edge devices were tested, with two types having several variations. The following is a list of these trailing-edge modifications including reference to sketches and photographs of each:

Trailing-edge modification	Ramp angle, deg	Figure number
Triangular wedges		
Short chord	0	3(a) and 4(a)
Short chord	3-1/2	3(b) and 4(b)
Long chord	0	3(c) and 4(c)
Solid spanwise wedges		
Blunt trailing edge	3	3(d) and 4(d)
Splitter plate	3	3(e) and 4(e)
Parabolic shaped wedges	0	3(f) and 4(f)

RESULTS AND DISCUSSION

The zero-lift drag coefficients of the six trailing-edge modifications and the basic model are presented in figure 5. The drag increment, due to the various trailing-edge modifications, expressed as a percent, is shown in figure 6.

The Effect of Triangular Wedges

It can be seen in figure 6 that the addition of the short-chord wedges with a 0° ramp angle increased the drag approximately 20 percent over the value for the basic model in the subsonic Mach number range. This increment was slightly lower in the higher speed range. Increasing the ramp angle of the wedges to $3\text{-}1/2^\circ$ resulted in an 80-percent increase in drag in the subsonic Mach number range; again there was a reduction in the drag increment at the higher Mach numbers.

The effect of wedge chord can be seen by comparing the long-chord and short-chord triangular-wedge modifications with a 0° ramp angle. The drag increments are approximately the same for both modifications up to 0.87 Mach number, but the long-chord wedges had a greater drag rise throughout the transonic Mach number range. The transonic drag rise of the wedges might be substantially reduced by a properly contoured body. To explore this possibility the method of reference 4 was used to compute the transonic drag rise for the short- and long-chord wedges (ramp angle = 0°) and for the basic model for a Mach number of 1.05. These computed drag increments were added to the zero-lift subsonic drag. The relatively good agreement with measured total drag for this Mach number is shown in figure 5. Since the transonic drag rise can be computed by the linear theory of reference 4, it follows that similar computational methods could be used to recontour the body shape so as to essentially eliminate the transonic drag rise due to the various wedges.

The Effect of Solid Spanwise Wedges

Examination of figure 6 shows that the blunt trailing-edge modification gave the largest drag rise of all the modifications presented at both subsonic and supersonic Mach numbers (drag rise was approximately 325 and 140 percent, respectively).

Removing the rear 50 percent of the blunt trailing-edge modification, thus forming a splitter plate, reduced the drag increment to approximately 125 percent in the subsonic Mach number range.

The Effect of Parabolic Shaped Wedges

In order to determine the effect of wedge shape on the drag, wedges having a parabolic plan form were constructed. Each parabolic shaped wedge occupied about the same volume and had the same ramp angle (0°) as the short-chord triangular wedge it replaced. Figure 6 shows that changing the shape of the wedge had little effect on the drag increment throughout the range of the test.

Ames Aeronautical Laboratory
National Advisory Committee for Aeronautics
Moffett Field, Calif., April 15, 1958

REFERENCES

1. Wyss, John A., Sorenson, Robert M., and Gambucci, Bruno J.: Effects of Modifications to a Control Surface on a 6-Percent-Thick Unswept Wing on the Transonic Control-Surface Flutter Derivatives. NACA RM A58B04, 1958.

2. Moseley, William C., Jr., and Price, George W., Jr.: Effects of Control Profile on the Oscillating Hinge-Moment and Flutter Characteristics of a Flap-Type Control at Transonic Speeds. NACA RM L57E27, 1957.

3. Holdaway, George H., and Hatfield, Elaine W.: Investigation of Symmetrical Body Indentations Designed to Reduce the Transonic Zero-Lift Wave Drag of a 45° Swept Wing With an NACA 64A006 Section and With a Thickened Leading-Edge Section. NACA RM A56K26, 1957.

4. Holdaway, George H., and Mersman, William A.: Application of Tchebichef Form of Harmonic Analysis to the Calculation of Zero-Lift Wave Drag of Wing-Body-Tail Combinations. NACA RM A55J28, 1956.

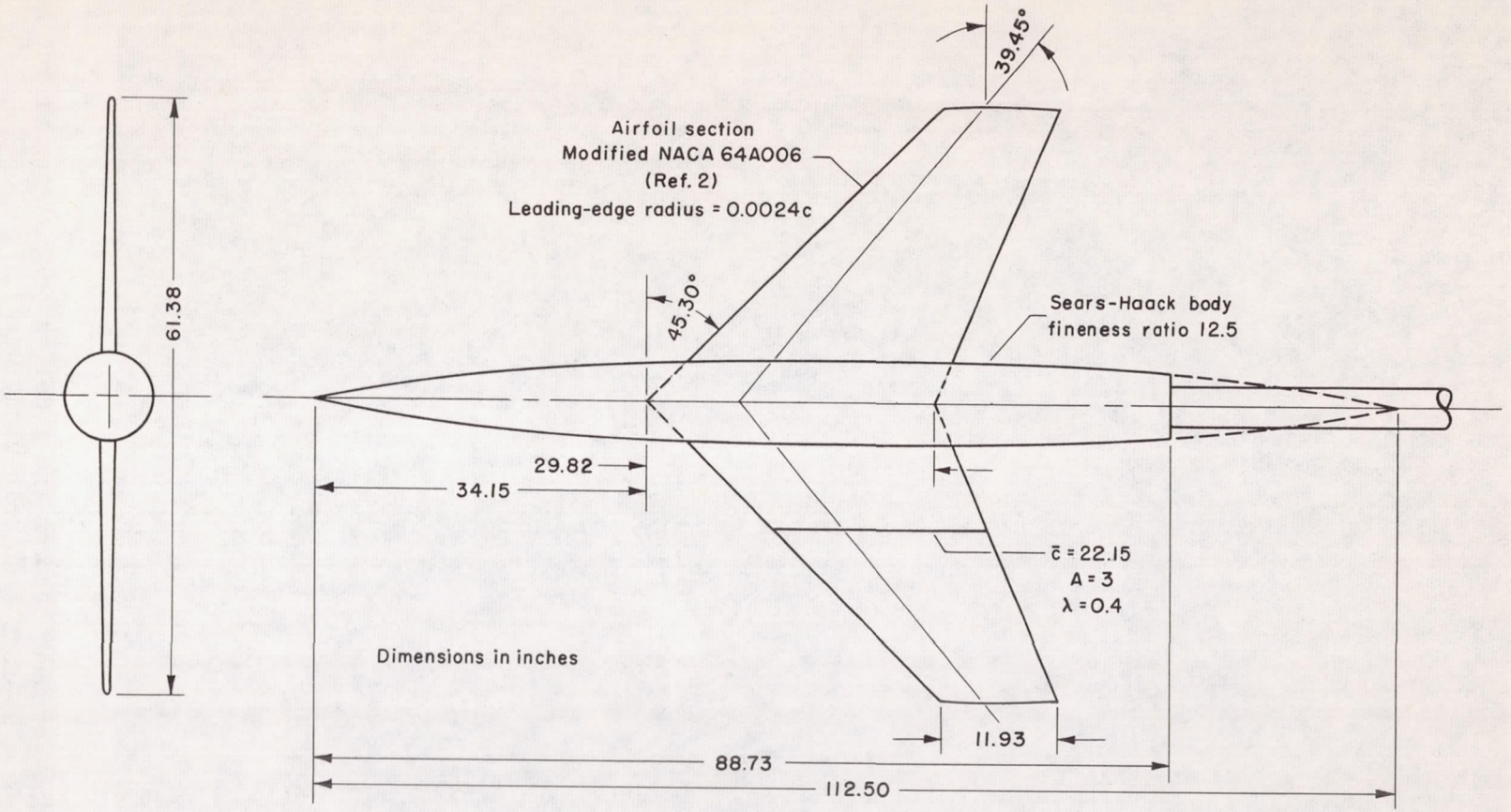

Figure 1.- Sketch of basic wing-body combination.

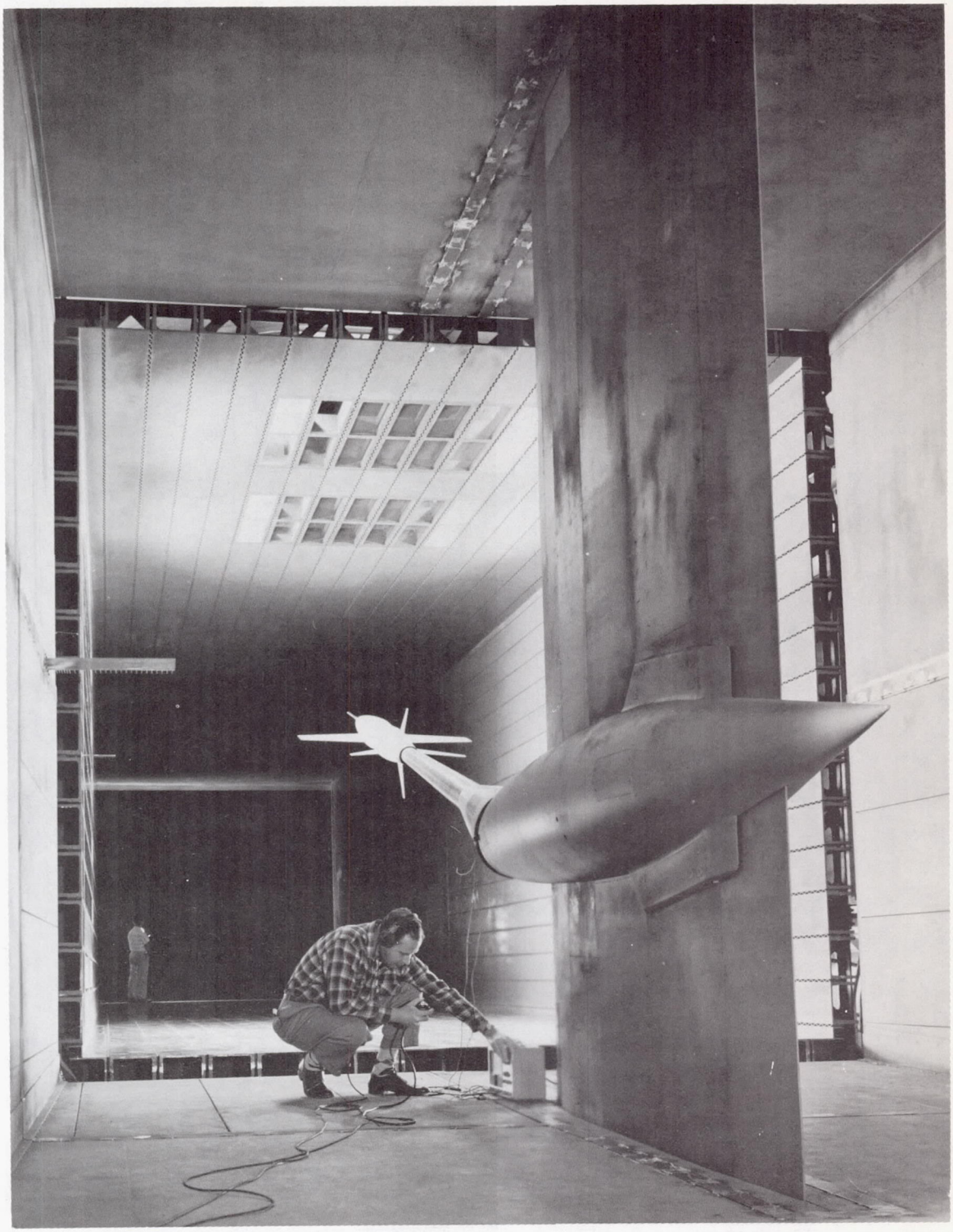

A-20417

Figure 2.- Rear view of test section and model support system of the Ames 14-foot transonic wind tunnel.

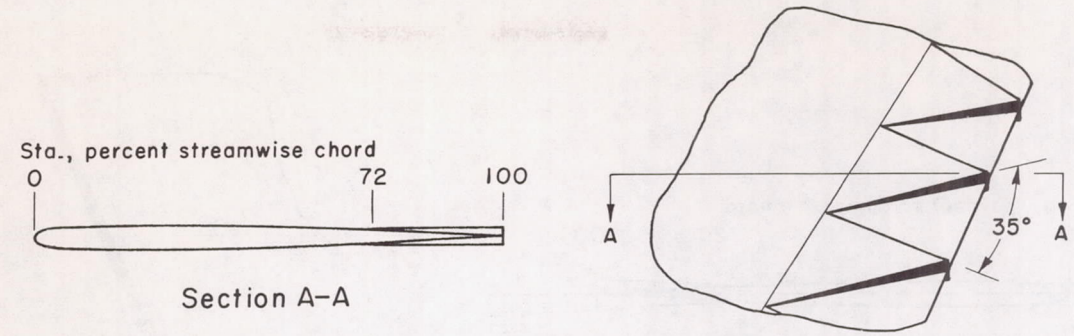

(a) Short-chord wedges; ramp angle = 0°.

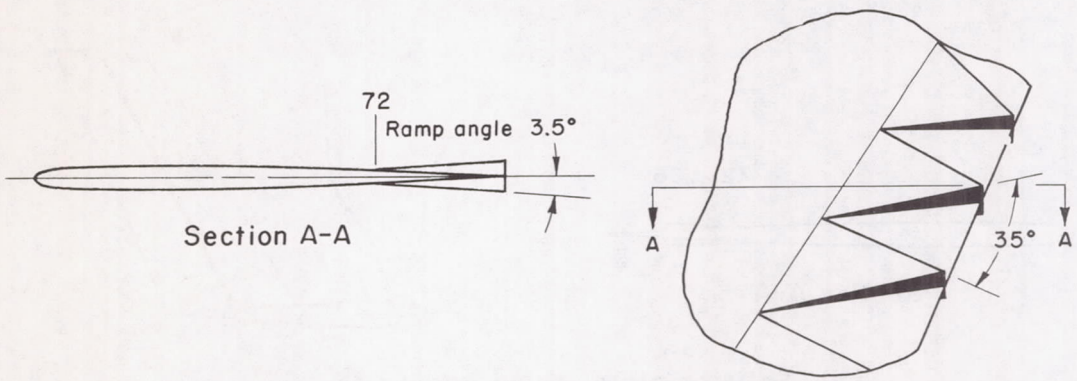

(b) Short-chord wedges; ramp angle = 3.5°

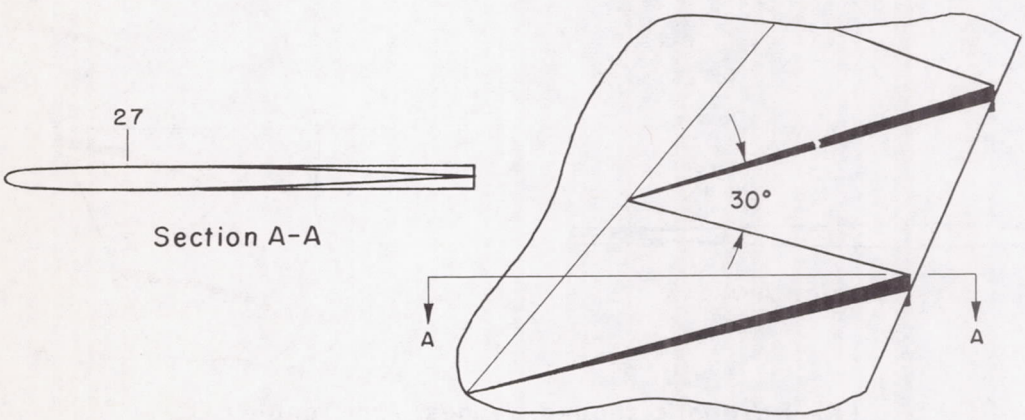

(c) Long-chord wedges; ramp angle = 0°.

Figure 3.- Sketches of wedge configurations.

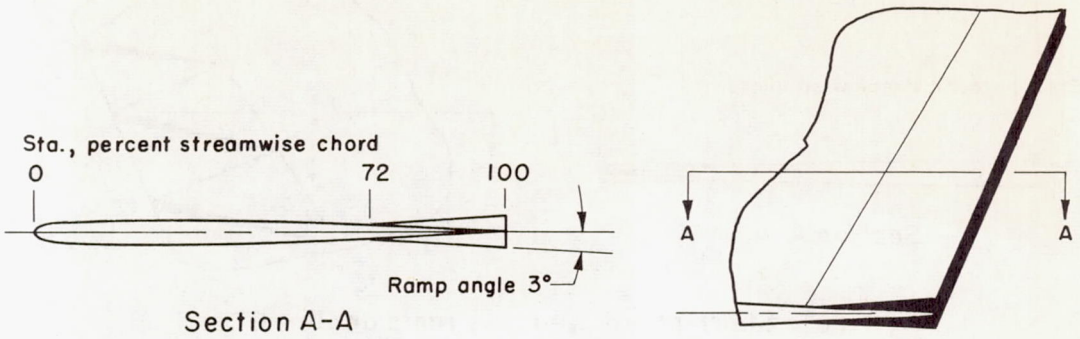

(d) Blunt trailing edge; ramp angle = 3°.

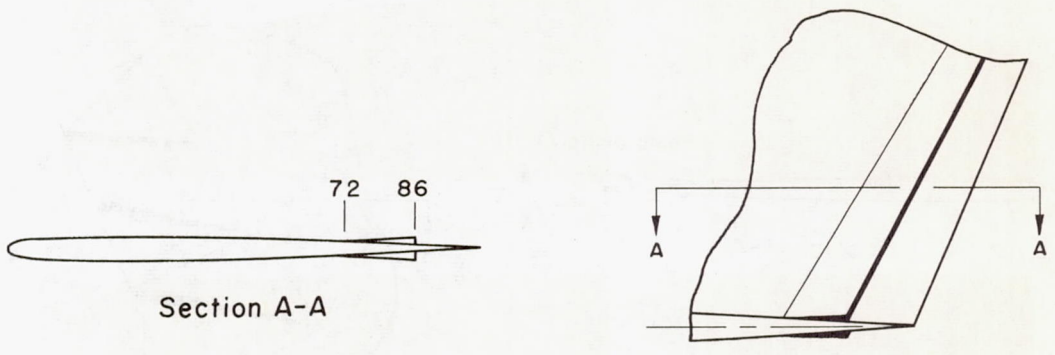

(e) Splitter plate; ramp angle = 3°

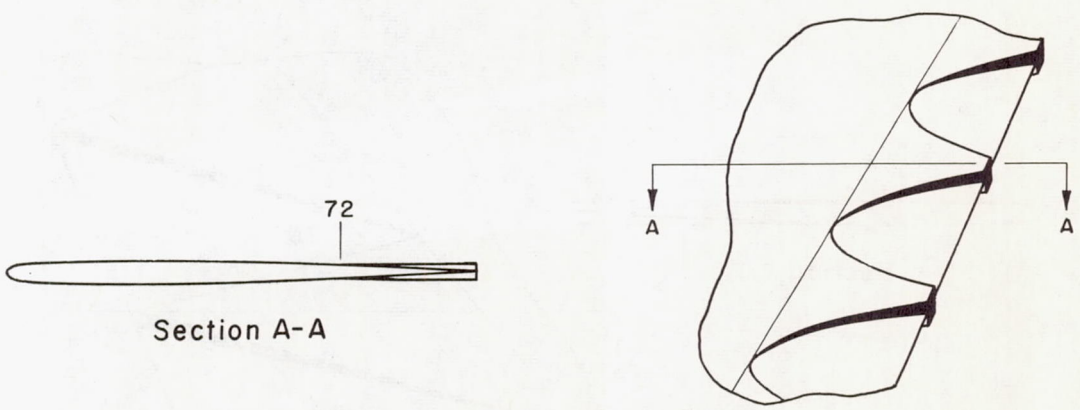

(f) Parabolic-shaped wedges; ramp angle = 0°.

Figure 3.- Concluded.

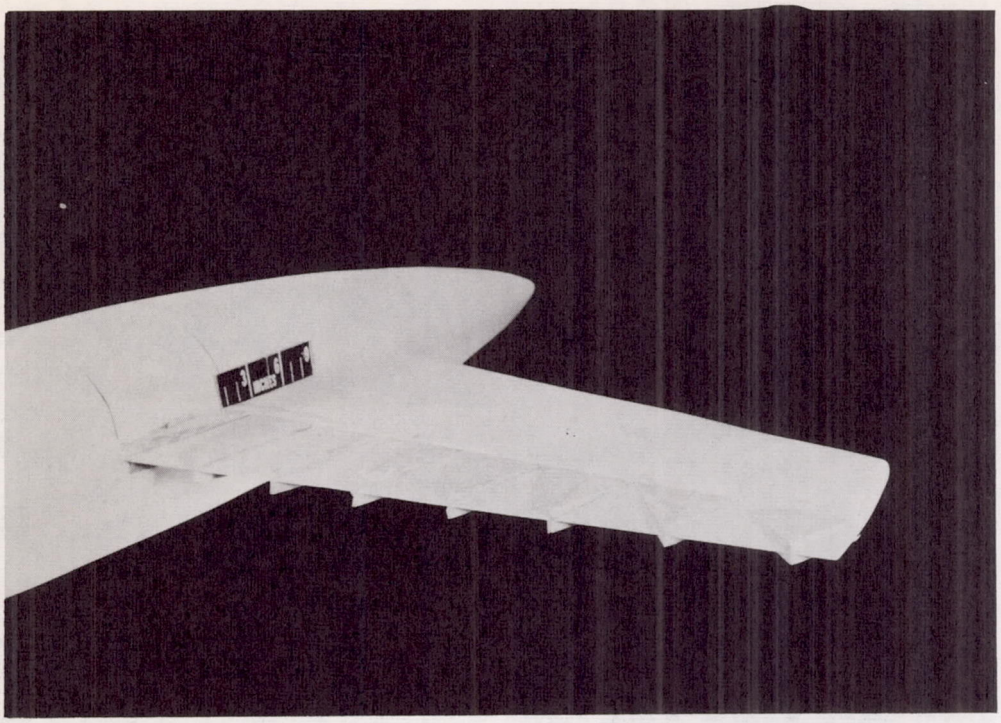

(a) Short-chord wedges; ramp angle = 0°. A-23175

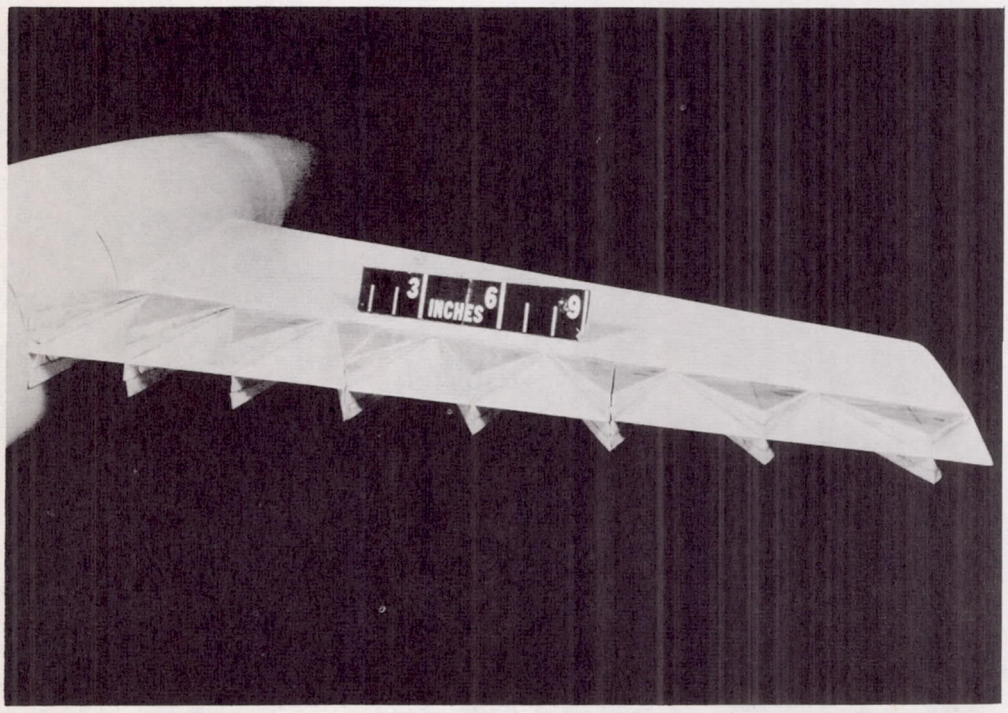

A-23160

(b) Short-chord wedges; ramp angle = 3-1/2°.

Figure 4.- Rear view of the model with various shaped wedges installed.

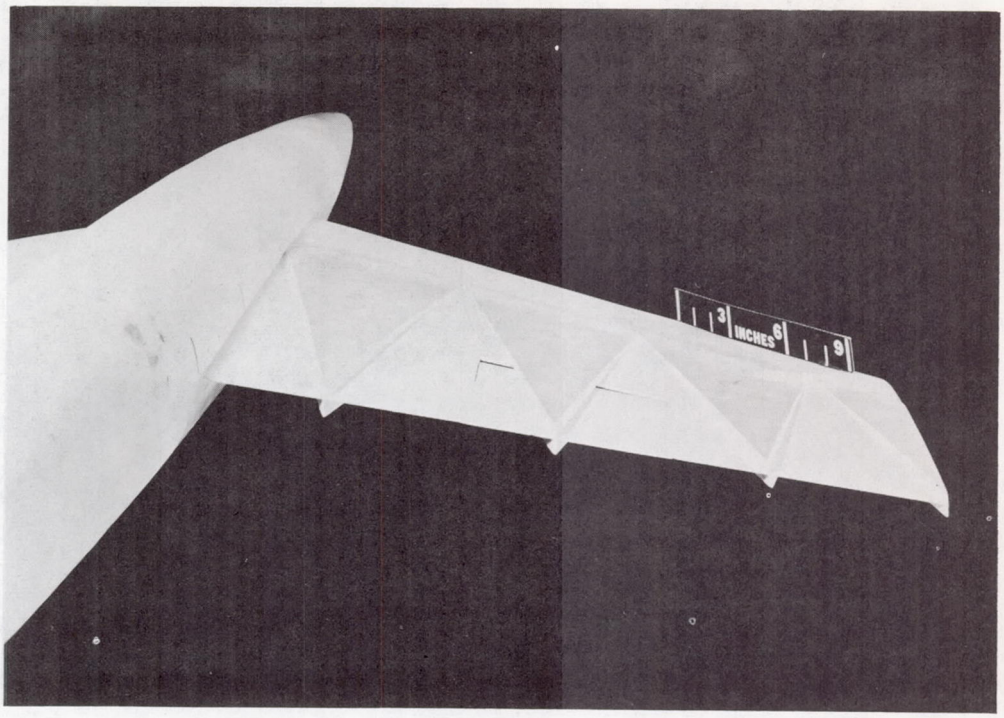

(c) Long-chord wedges; ramp angle = 0°. A-23192

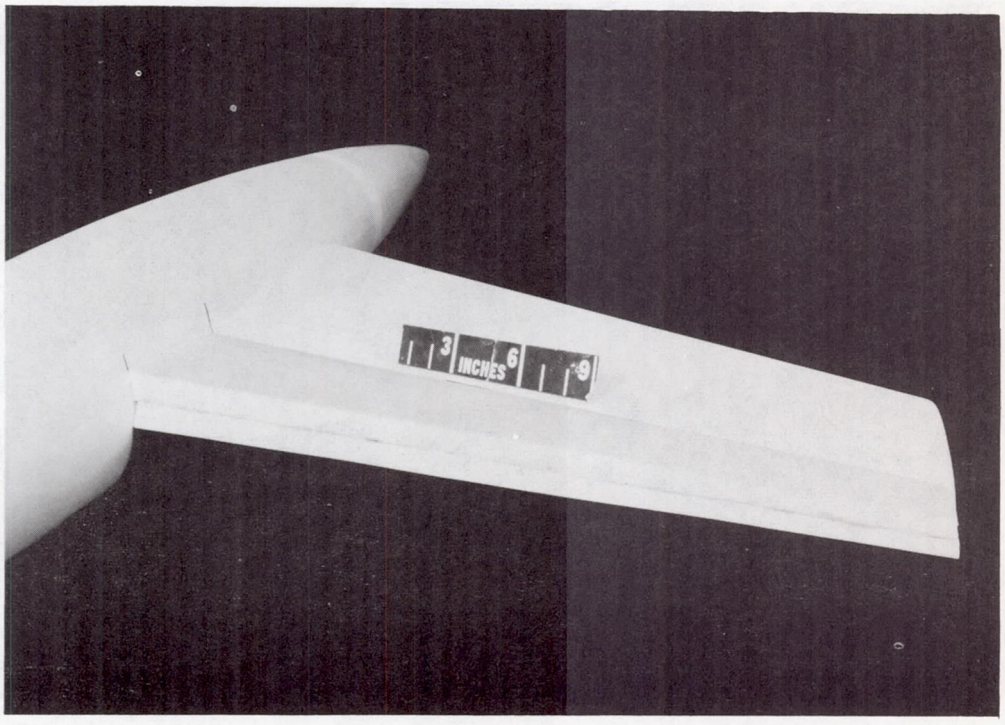

A-23184

(d) Blunt trailing edge; ramp angle = 3°.

Figure 4.- Continued.

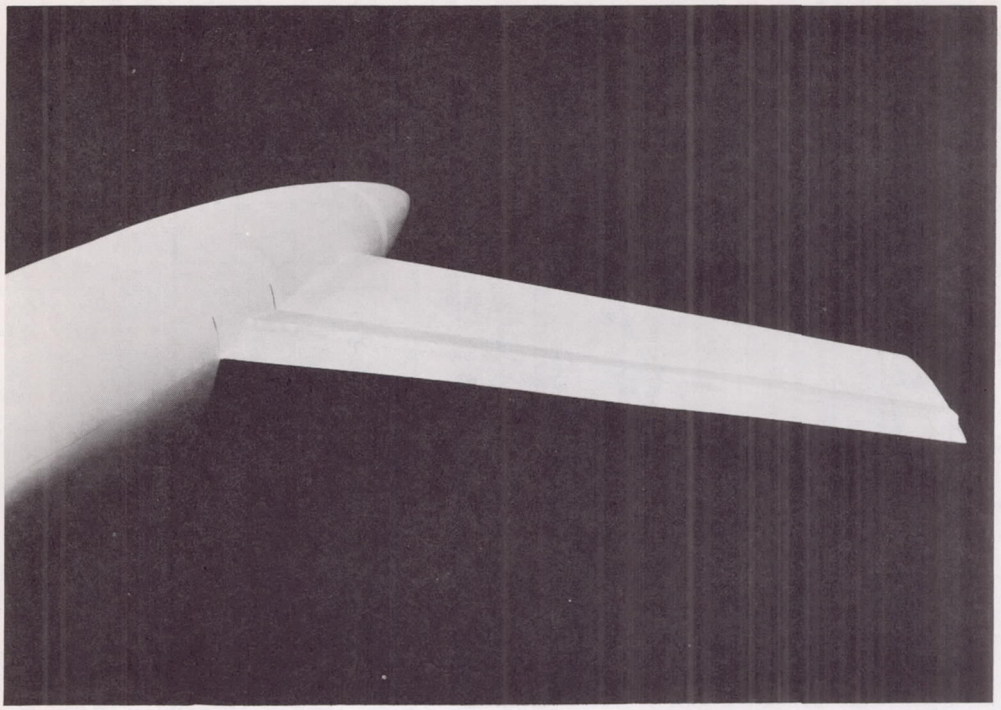

(e) Splitter plate; ramp angle = 3°. A-23187

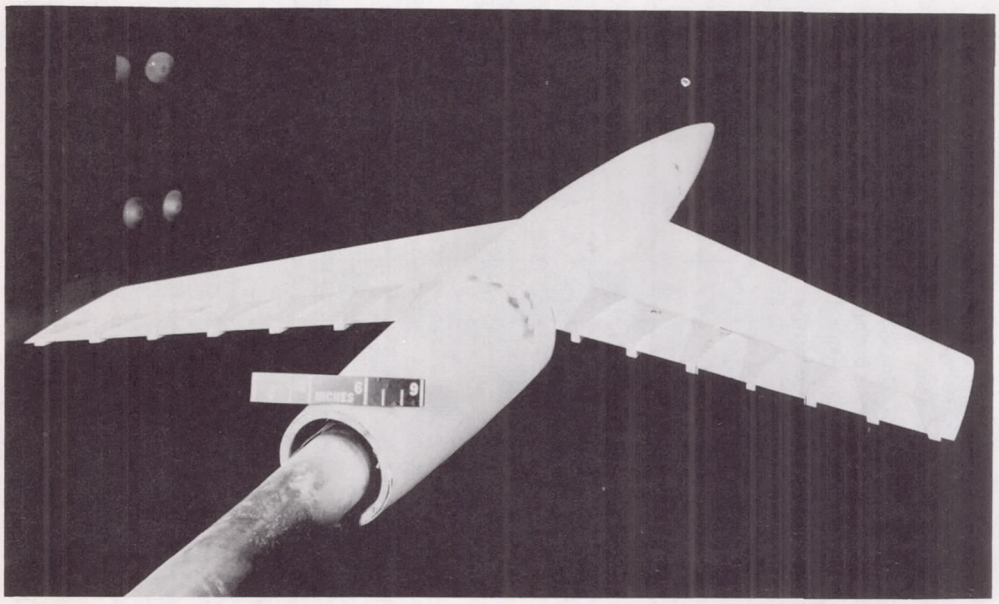

A-23195

(f) Parabolic-shaped wedges; ramp angle = 0°.

Figure 4.- Concluded.

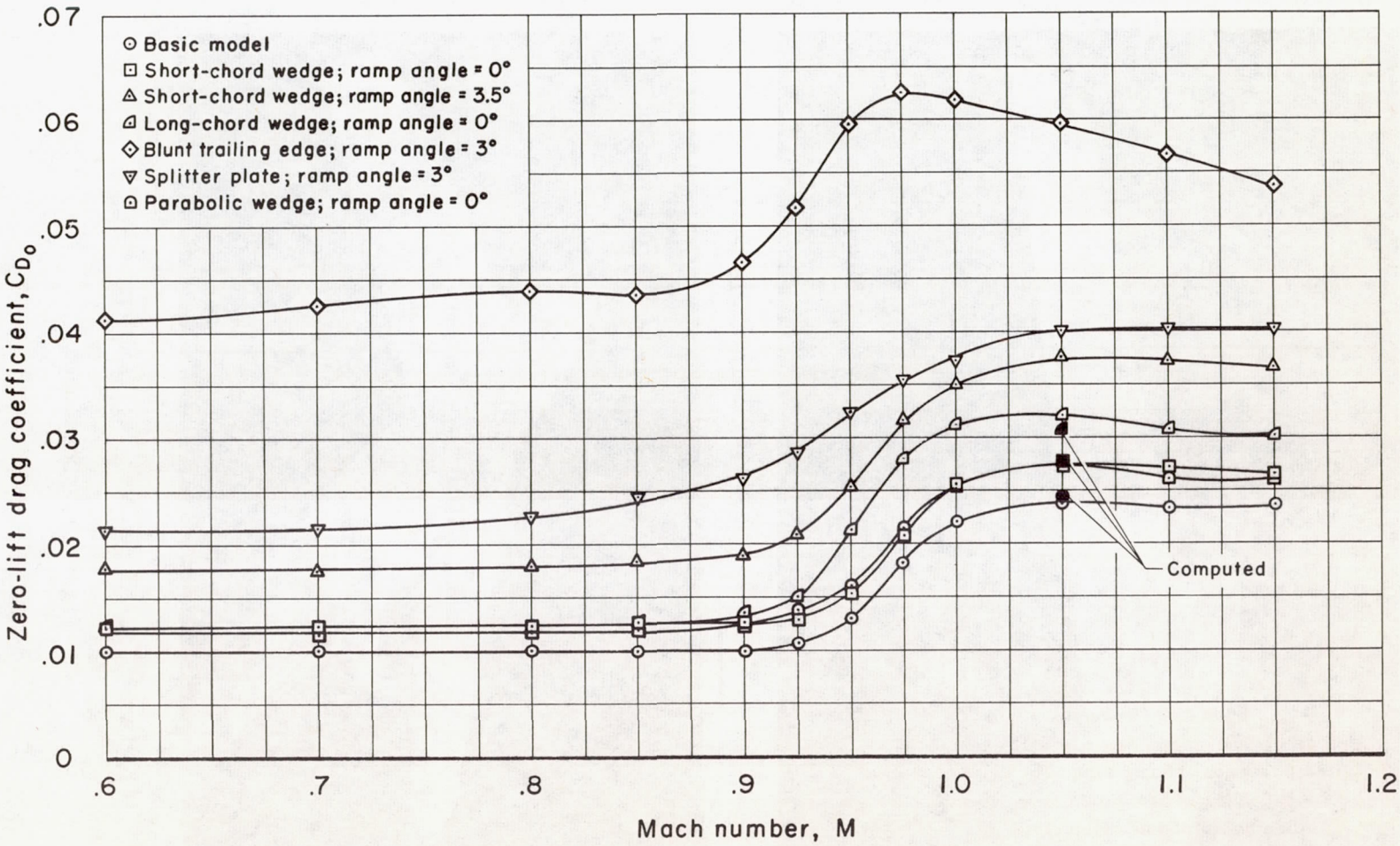

Figure 5.- Zero-lift drag variation for the various trailing-edge modifications.

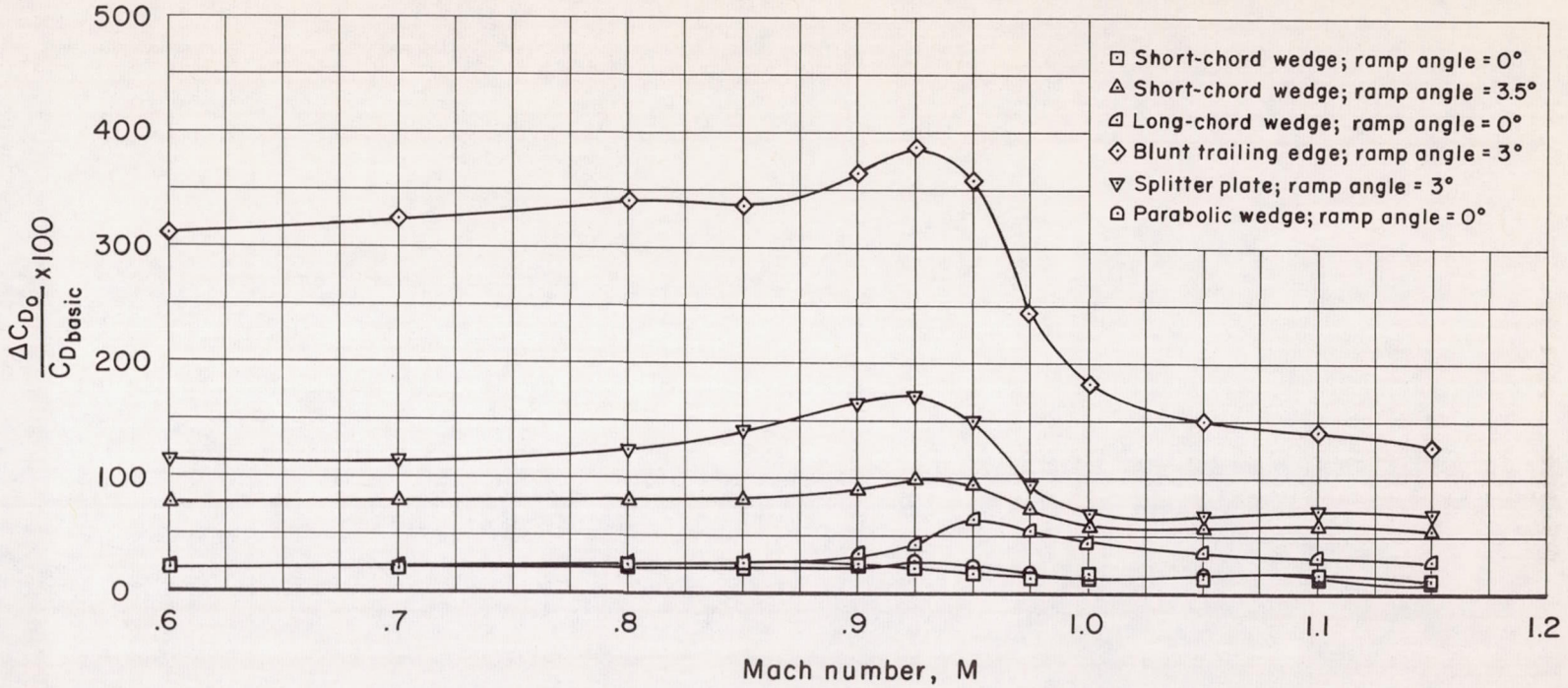

Figure 6.- Zero-lift drag increment due to the trailing-edge modifications.